**Legends for supplementary movies**

**Supplementary Movie 1**: Spontaneous whole-cell $Ca^{2+}$ oscillations from GFP-NRVMs loaded with rhod-2AM and recorded in the presence of a gap-junction uncoupler, palmitoleic acid (20μM). Complete gap-junction uncoupling demonstrates that spontaneous whole-cell $Ca^{2+}$ transients (and beating) are observed in only a few GFP-NRVMs.

**Supplementary Movie 2**: Spontaneous whole-cell $Ca^{2+}$ oscillations from Tbx18-NRVMs loaded with rhod-2AM and recorded in the presence of a gap-junction uncoupler, palmitoleic acid (20μM). Most Tbx18-NRVMs exhibit spontaneous whole-cell $Ca^{2+}$ transients beating independent from each other due to complete gap-junction uncoupling.

Supplementary Figure 1

A. neonatal rat SAN

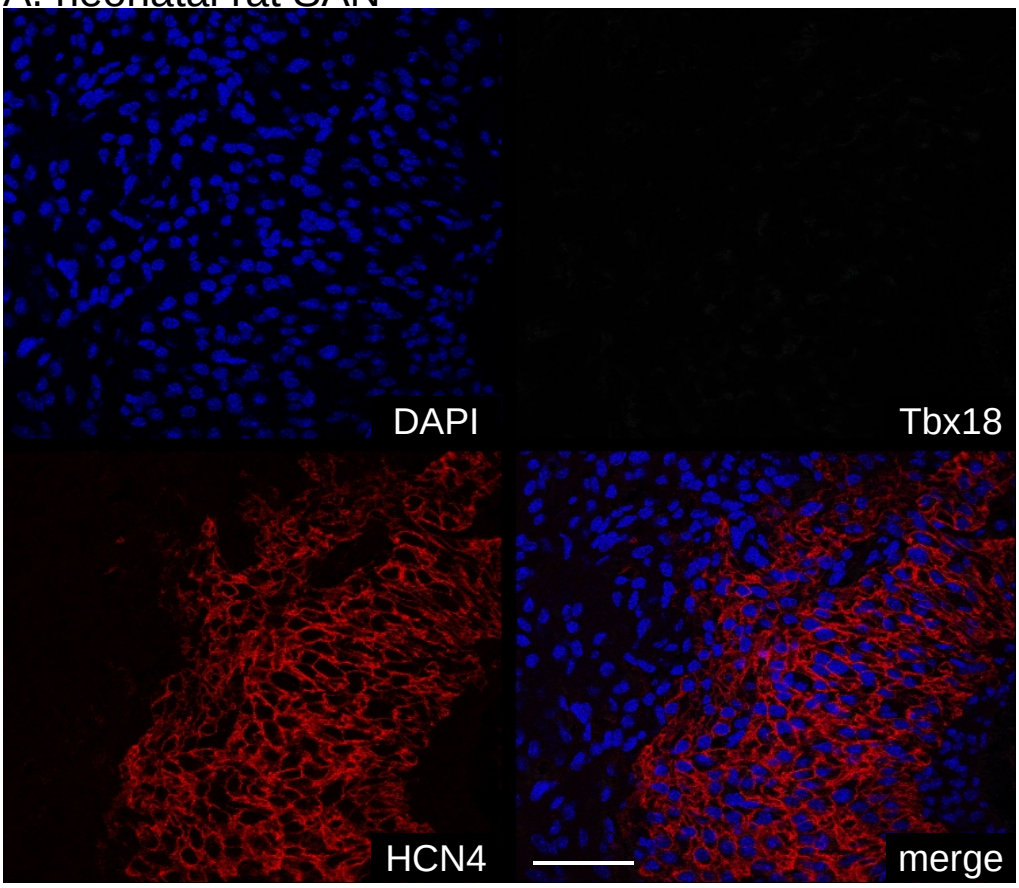


B. adult rat SAN

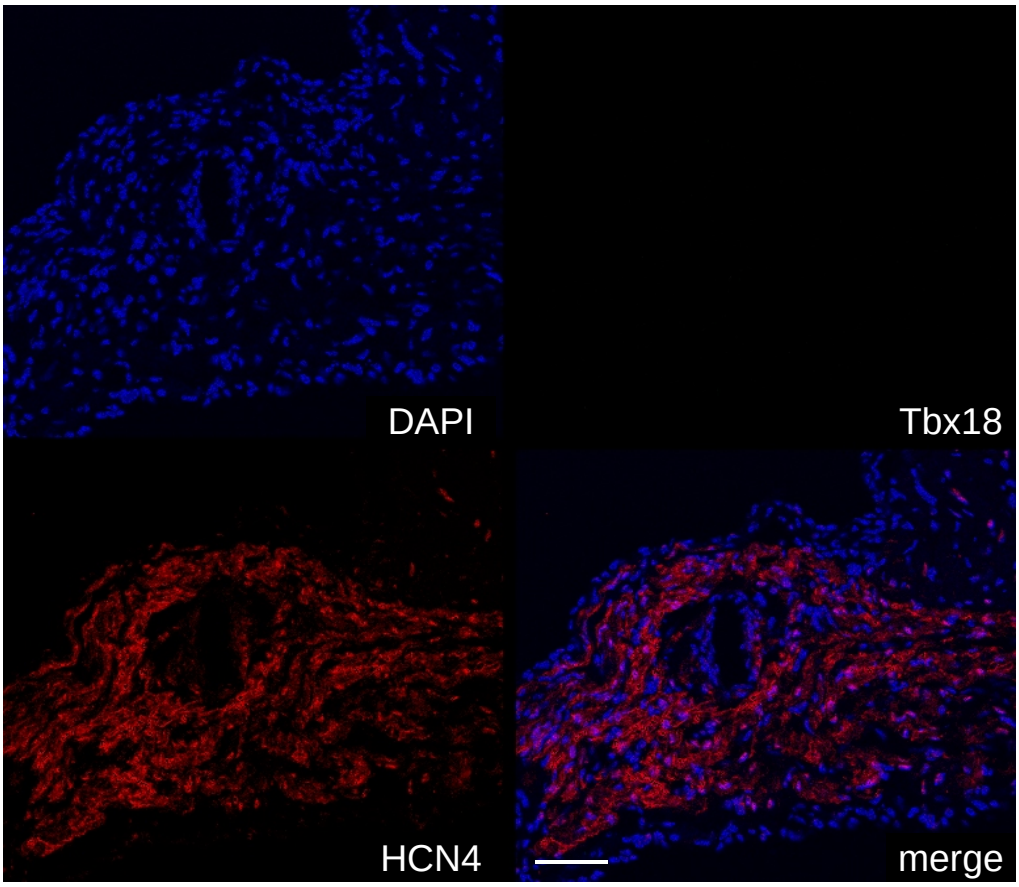

**Supplementary Figure 1**. Immunohistochemistry of neonatal (a) and adult (b) rat heart SAN, indicates that Tbx18 is undetectable in the postnatal SAN area. The SAN is demarcated by HCN4 co-staining and separated from the surrounding atria (bottom left of A and B). Scale bar: 50μm.

Supplementary Figure 2A

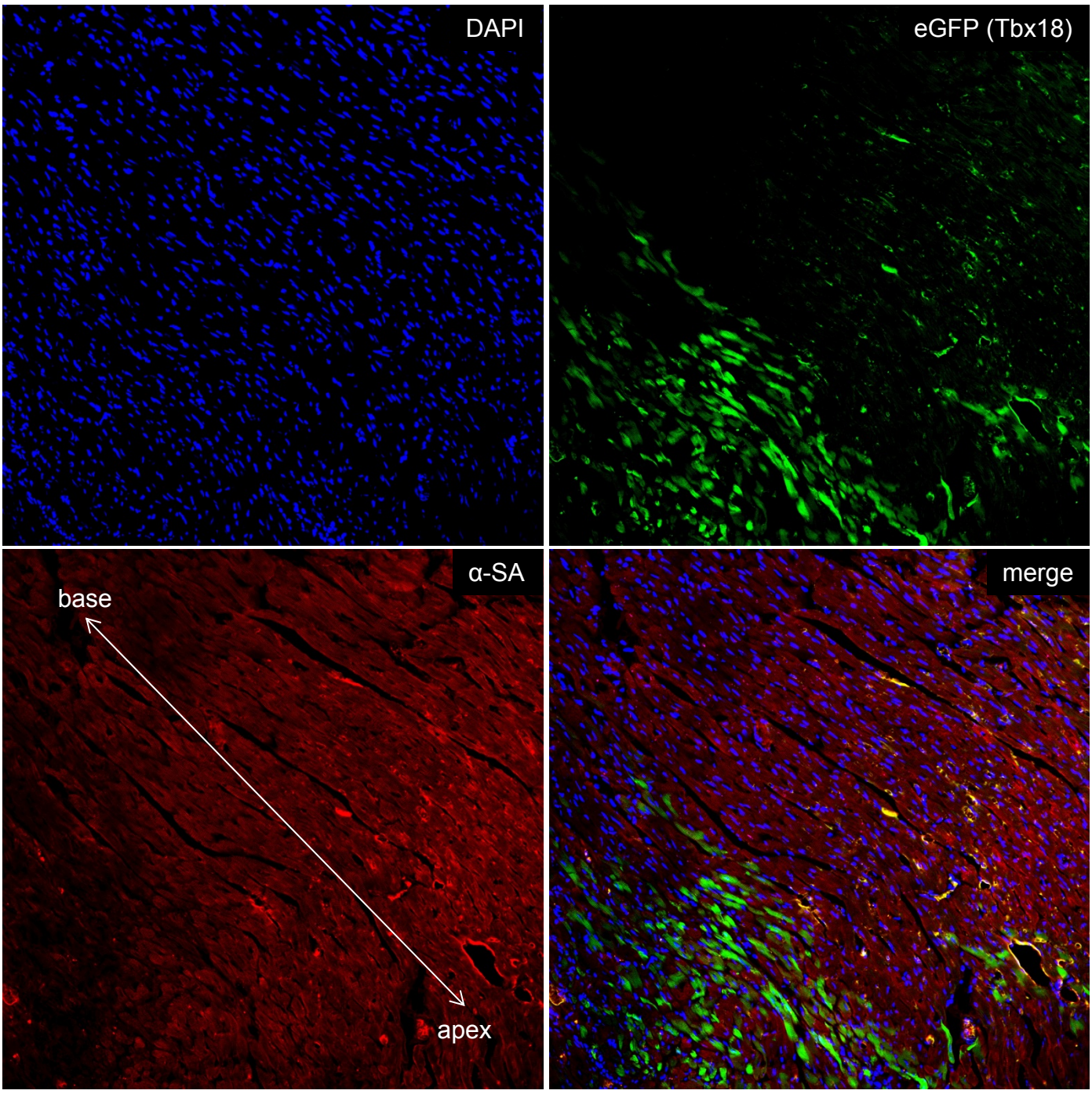

Supplementary Figure 2B

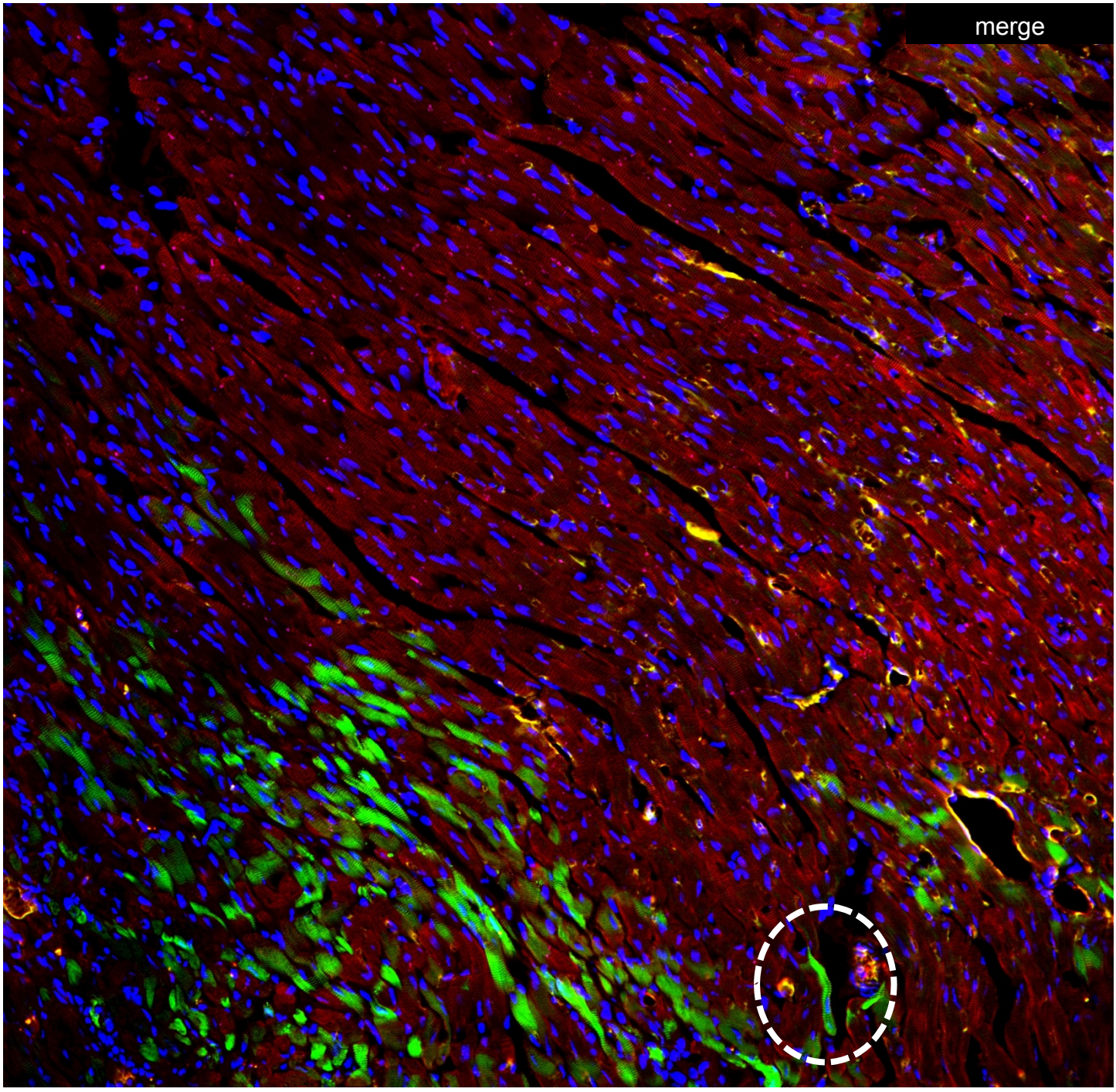

**Supplementary Figure 2.** Intramyocardial injection of adenoviral vector expressing Tbx18-IRES-eGFP into the left ventricular apex of the guinea pig heart leads to efficient and localized transduction (A).Tbx18 transduction was found near the apex of the heart. Leaner and smaller myocytes are visible in Tbx18-VMs, an example of which is highlighted by a white circle in (B).

Supplementary Figure 3

A. GFP-guinea pig

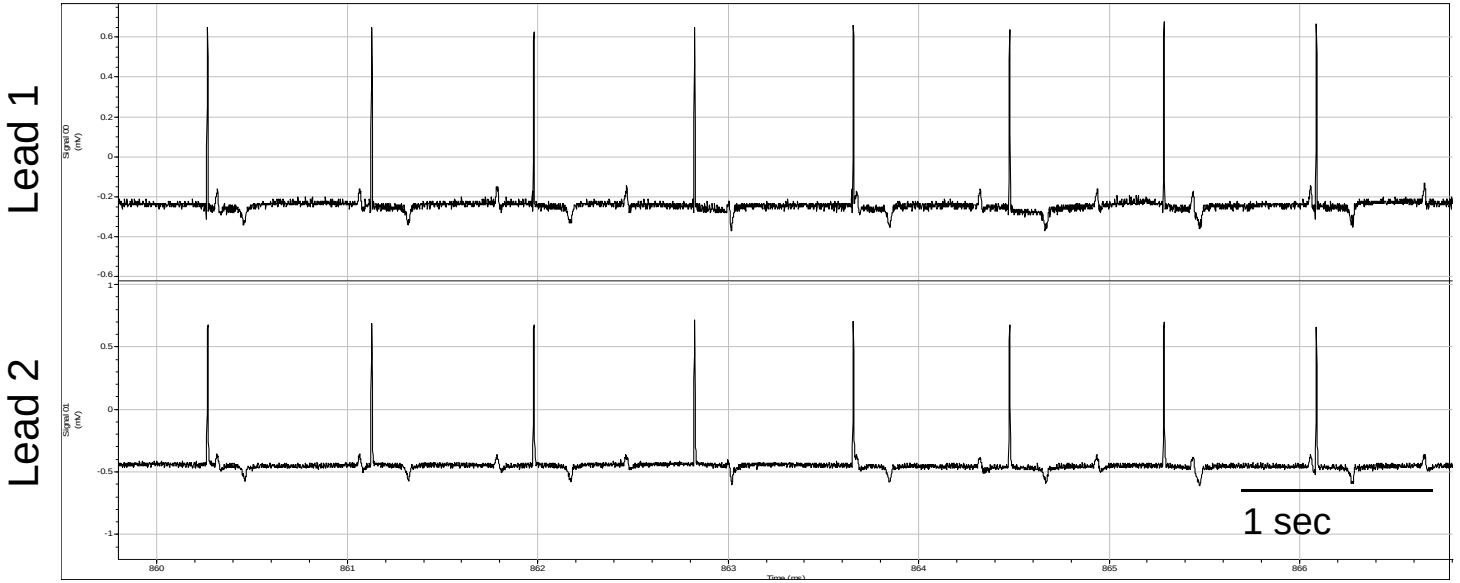


B. Tbx18-guinea pig

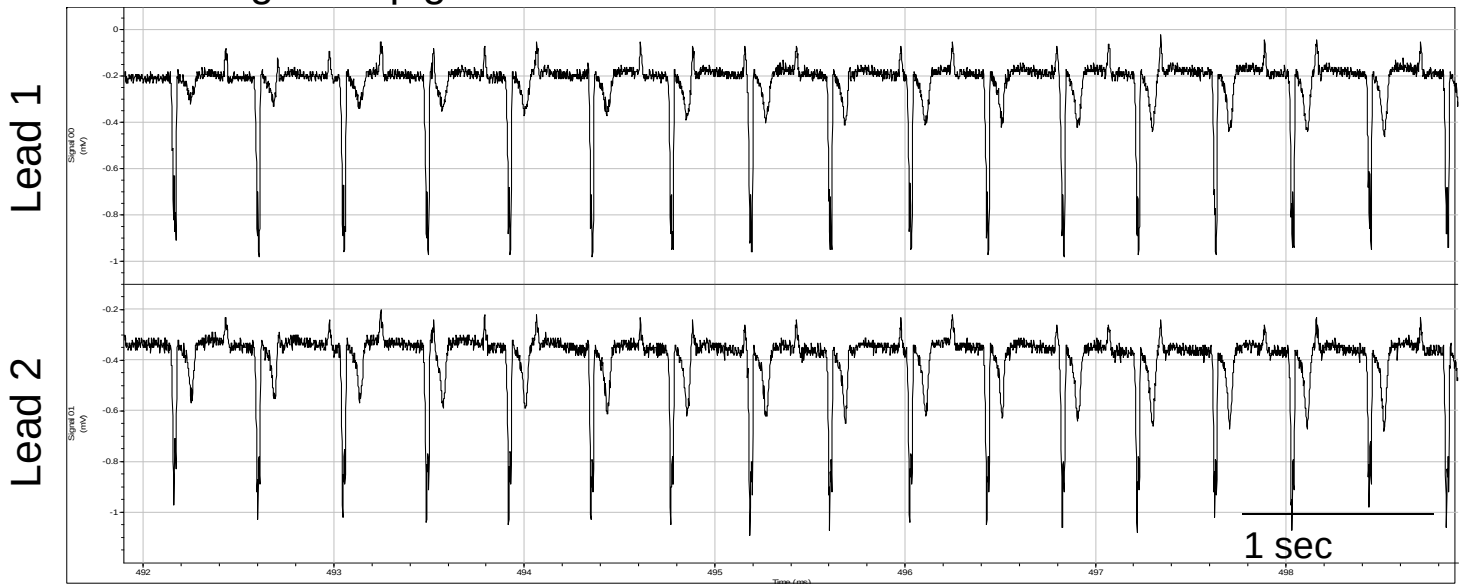

**Supplementary Figure 3.** Focal expression of Tbx18 in the apex of guinea pig hearts *in vivo* created ectopic ventricular beats. Representative electrocardiograms of Tbx18- or GFP- injected guinea pig (A and B, respectively). Downward (negative) deflection in ECG recording on lead II after methacholine injection (0.05mg/ml) revealed ectopic pacemaker activity originating from the ventricle with wide QRS complexes in Tbx18-injected guinea pigs (B). In contrast, GFP-injected guinea pigs (n=7) exhibited antegrade, junctional rhythm with narrow QRS complexes (A). No retrograde, ectopic beats with wide QRS complexes were observed in GFP-injected guinea pigs.

# Supplementary Figure 4

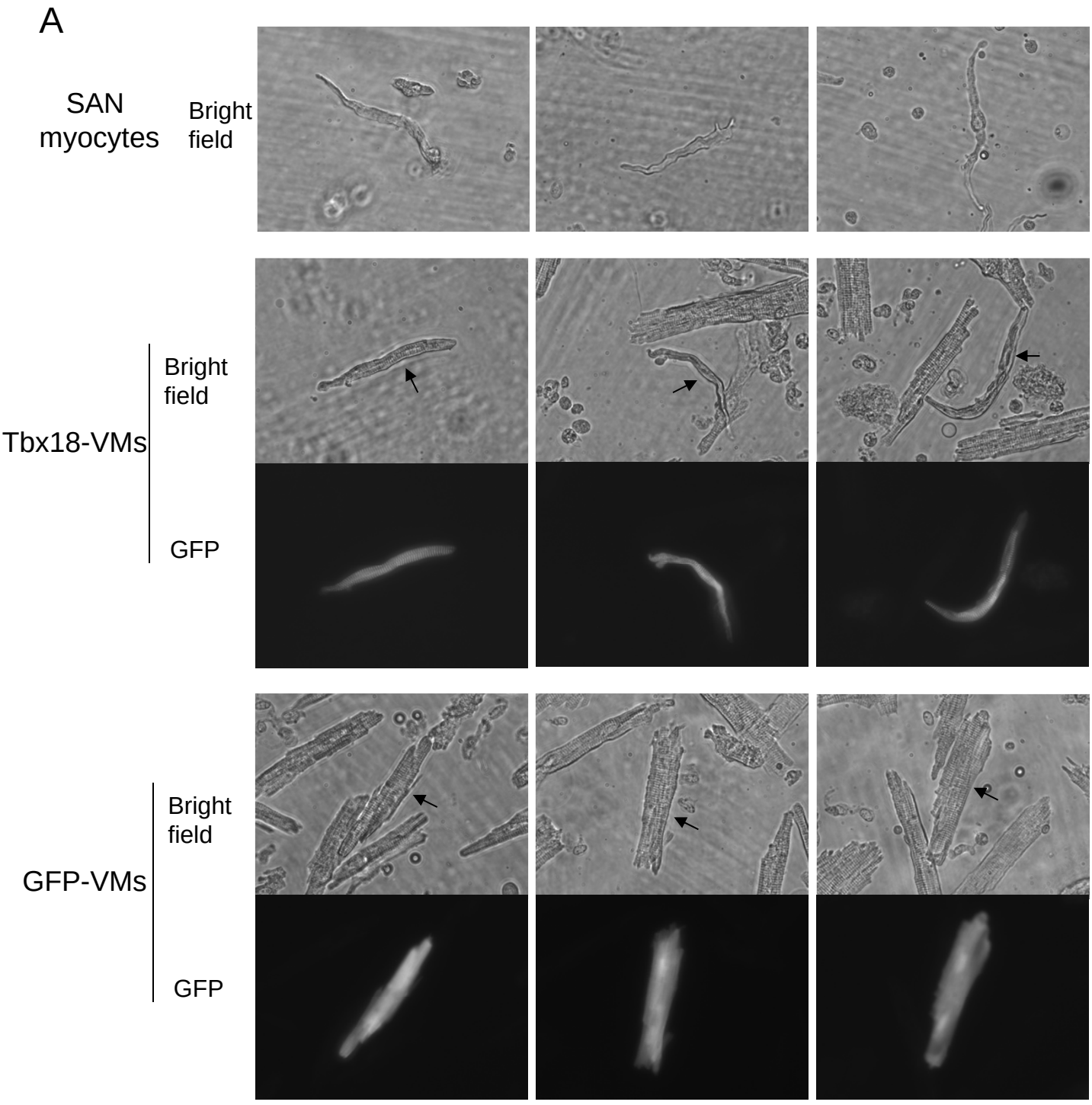


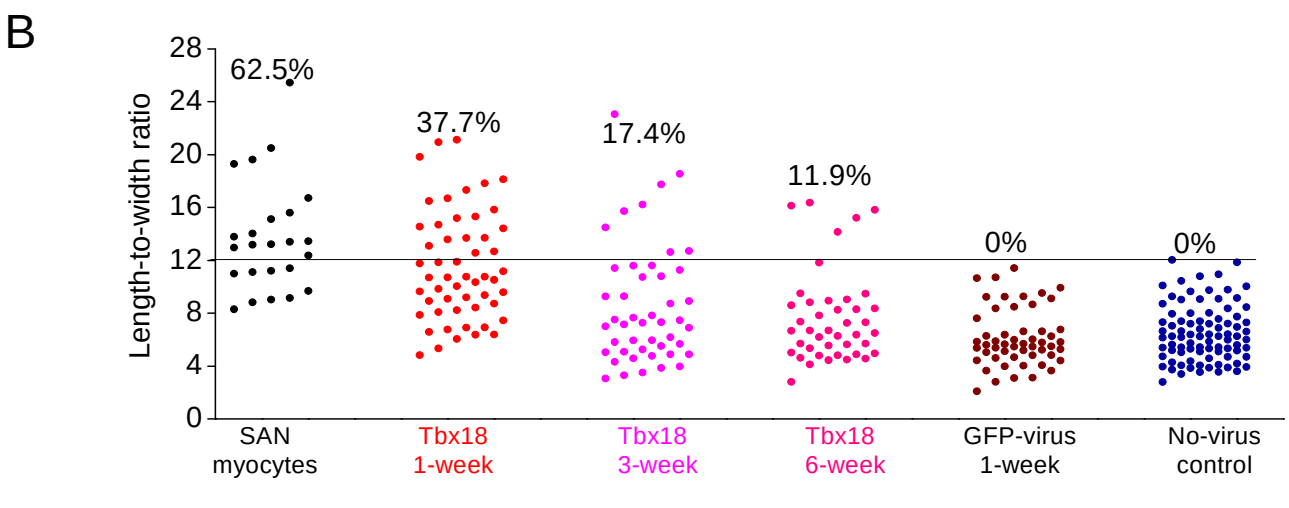

**Supplementary Figure 4**. Freshly-isolated Tbx18-VMs resemble the morphology of native SAN myocytes. **A**. Bright field images of native SAN myocytes (top panel) demonstrate tapered cell ends with leaner cell width which is recapitulated in Tbx18-VMs (middle panels with Tbx18-VMs marked by GFP fluorescence). In contrast, GFP-VMs maintain their brick-like shape (bottom panels). **B**. A scatter-plot of the length-to-width ratio. The myocytes were freshly isolated at the indicated time point. The width of each myocyte was determined by dividing the 2-dimensional surface area of each myocyte by its length.

Supplementary Figure 5

A

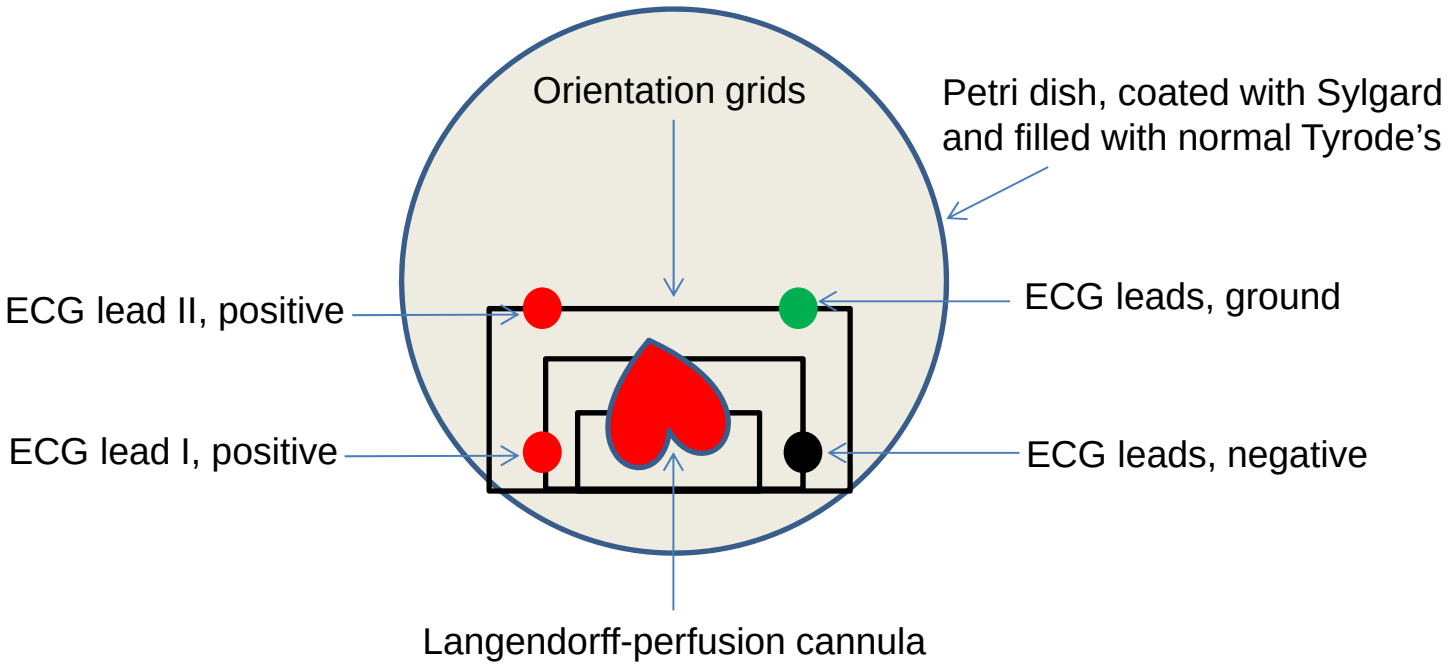


B

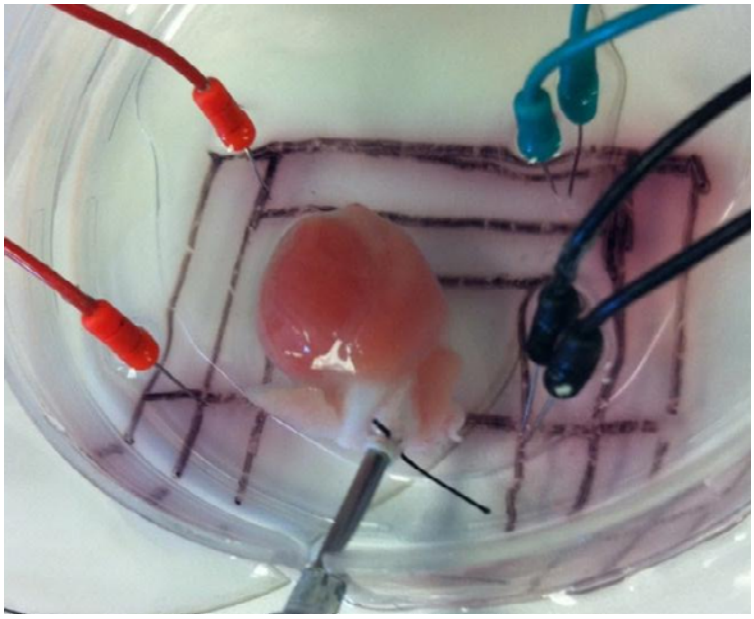

**Supplementary Figure 5**. *Ex vivo*, Langendorff-perfused heart set-up on which cryoablation was performed to create a model of complete heart block. **A**. Schematic representation of a cannulated heart with electrocardiographic recording leads for Lead I and II are indicated.. **B**. An actual perfused intact heart with its anterior side pointing up. The leads for electrocardiograph recording are inserted into Sylgard. Efforts were made to maintain consistent orientation of the heart and the ECG recording electrodes for all experiments.

Supplementary Figure 6

# Tbx18-heart (3-week)

A

idioventricular rhythm

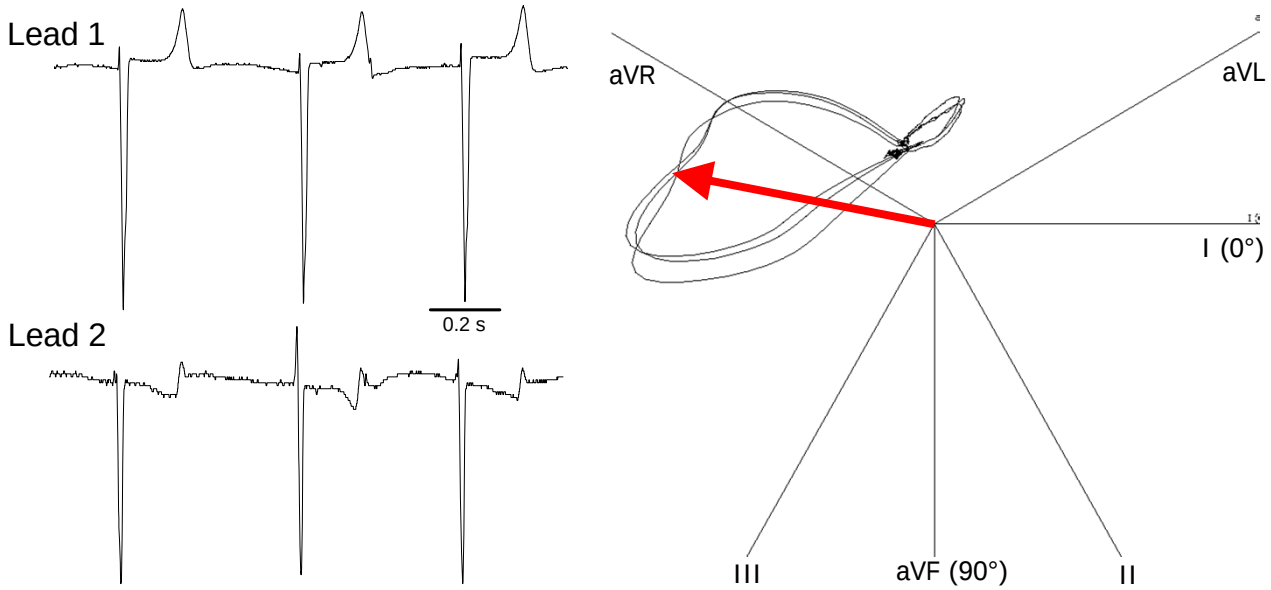


B

Paced at the injection site (LV apex)

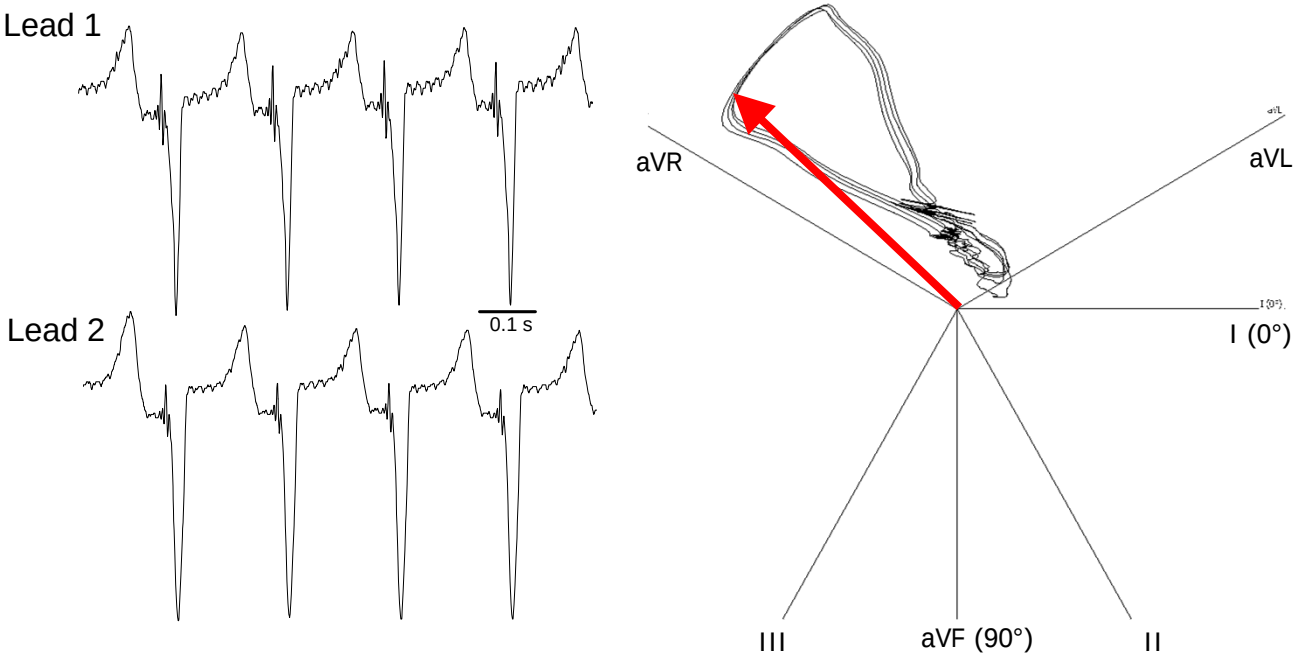


C

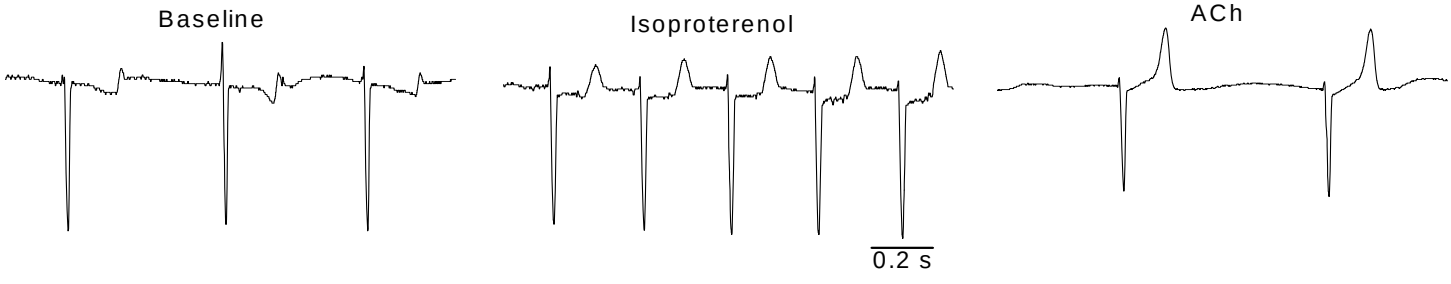

**Supplementary Figure 6**. Electrocardiographs from long-term Tbx18-injected heart demonstrate biological pacing originated from the site of Tbx18 injection. **A**. Electrocardiographic recordings of an intact perfused heart injected with Tbx18 at the apex. Tbx18 was directly injected into the apex of a guinea pig heart *in vivo*. Four weeks post-injection, the heart was harvest, perfused, and cryoablated at the AV junctional region. The polarity and morphology of the ectopic beats (**A**) is identical to those of electrode-paced beats at the site of transgene injection (**B**). **C**. Chronotropic response of the long-term Tbx18-injected heart to autonomic inputs was assessed by changing the perfusate (normal Tyrode's solution) to one that containing 1 μM isoproterenol for β-adrenergic stimulation followed by one that containing 1 μM acetylcholine for cholinergic suppression.

Supplementary Figure 7

Ad-eGFP

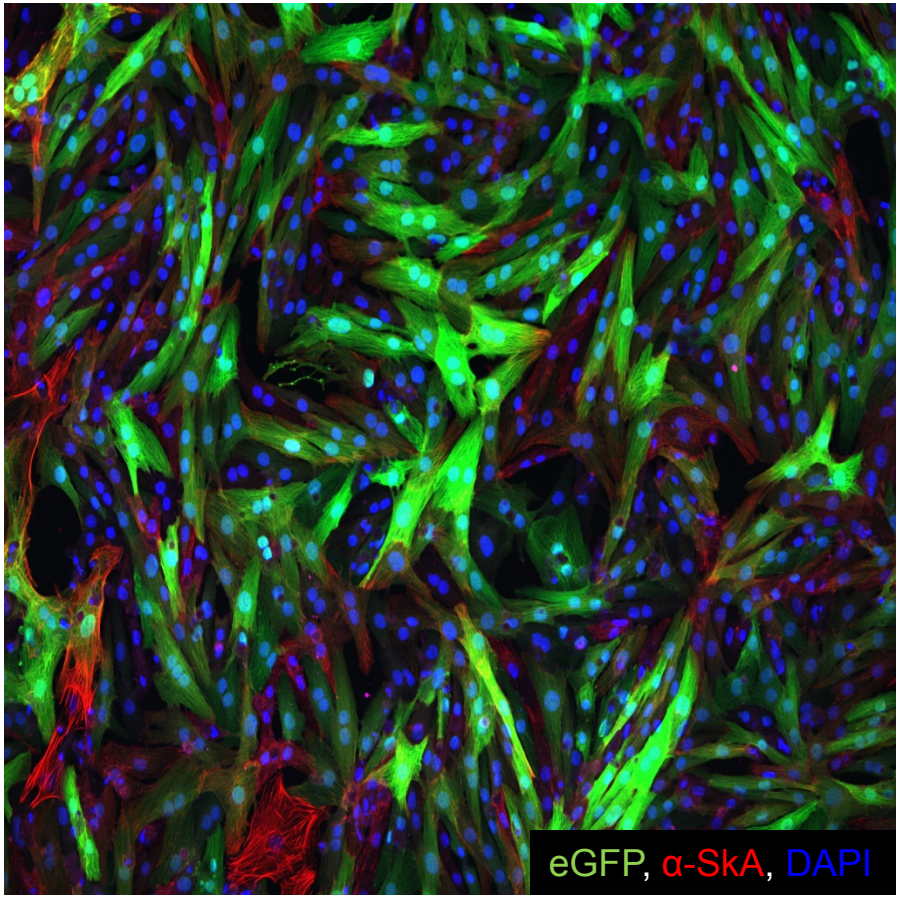


Ad-Tbx18-IRES-eGFP

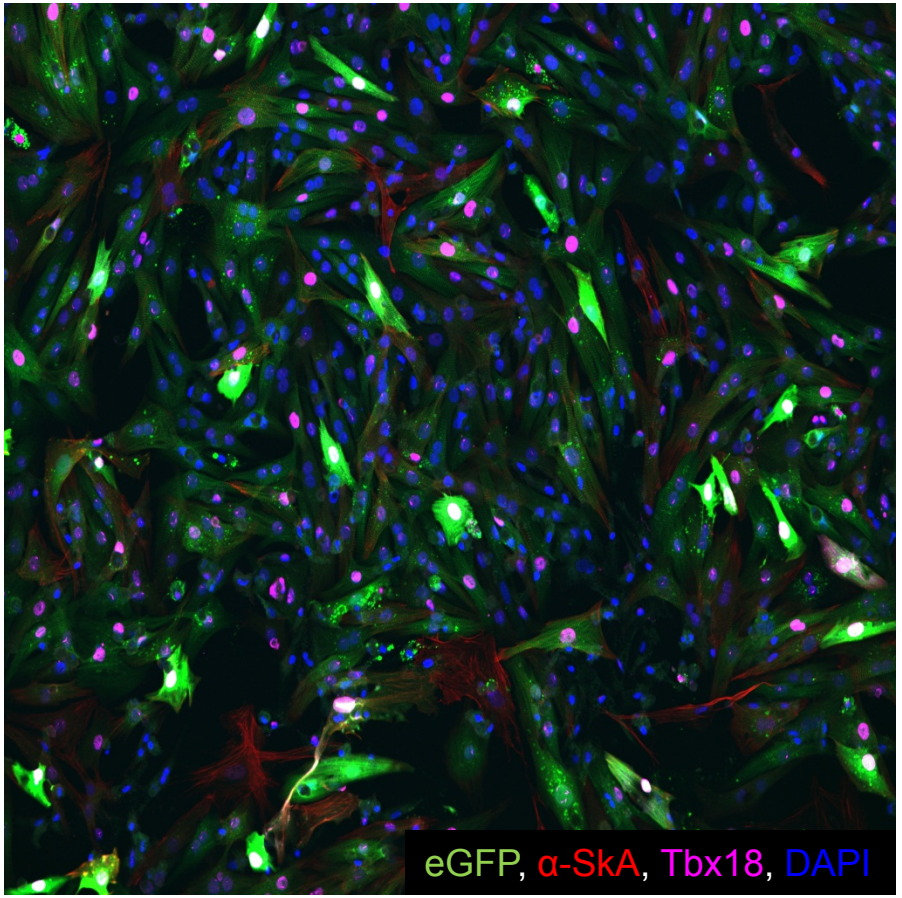

**Supplementary Figure 7.** Tbx18 re-expression does not lead to fetal gene expression as reported by α-skeletal actin.

Supplementary Figure 8

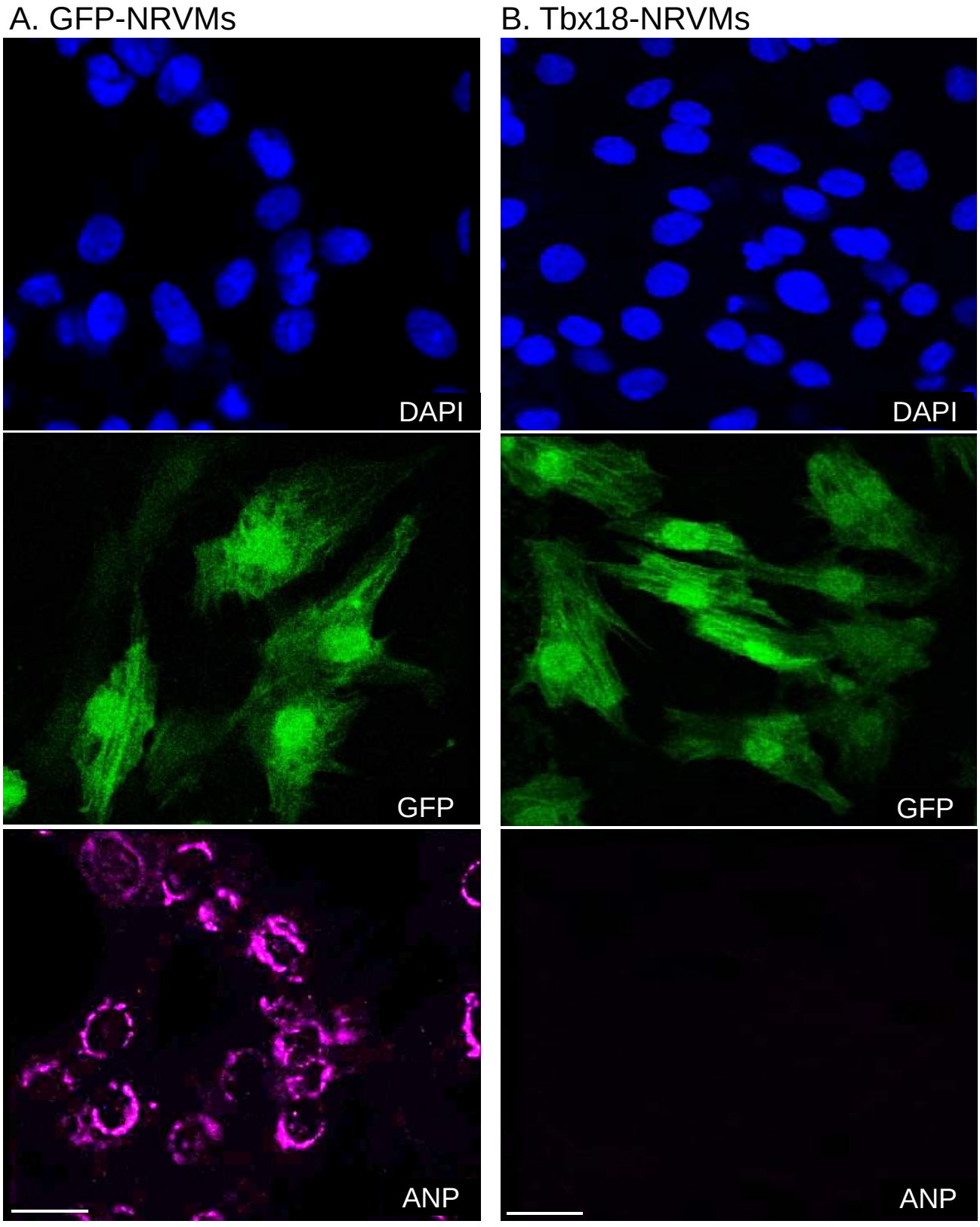

**Supplementary Figure 8.** Tbx18 strongly suppresses ANP expression. Expression of atrial natriuretic peptide (ANP) in NRVMs was induced by 24-hour stimulation with endothelin-1 (100 nM). Such ANP expression was suppressed by Tbx18 expression (B, bottom panel). Scale bar: 20μm.

Supplementary Figure 9

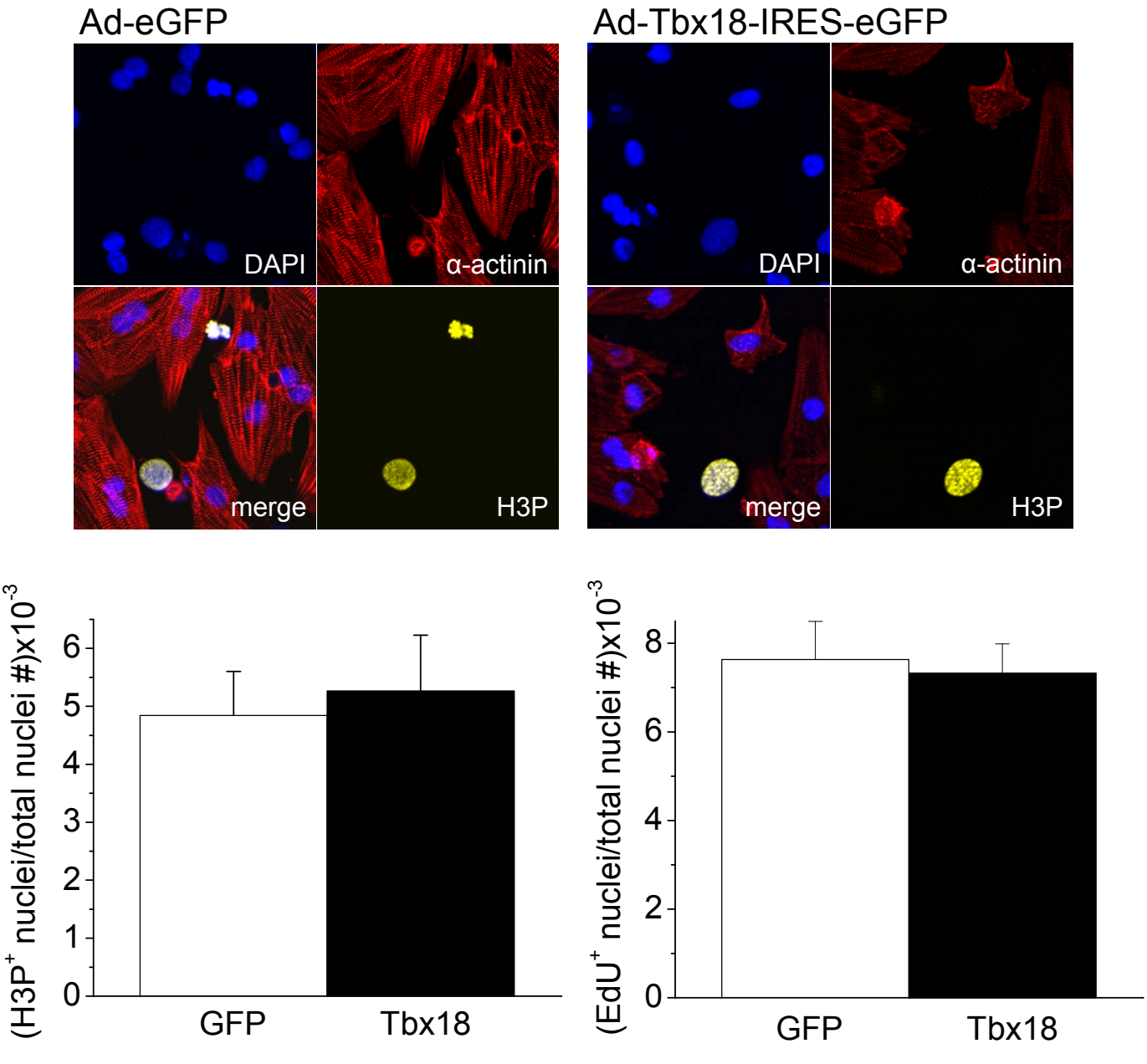

**Supplementary Figure 9.** Tbx18 re-expression does not lead to increase in the proliferative index in Tbx18-NRVMs as reported by percentages of H3P- or EdU-positive nuclei. The incidence of $H3P^+$ nuclei or $EdU^+$ nuclei were counted among total $DAPI^+$ nuclei. An average of three measurements is reported by analyzing images from three wells from an 8-chamber culture dish.

Supplementary Figure 10

Epigenetic Chromatin Remodeling Factors: RT-PCR array

A Tbx18-NRVMs vs. GFP-NRVMs

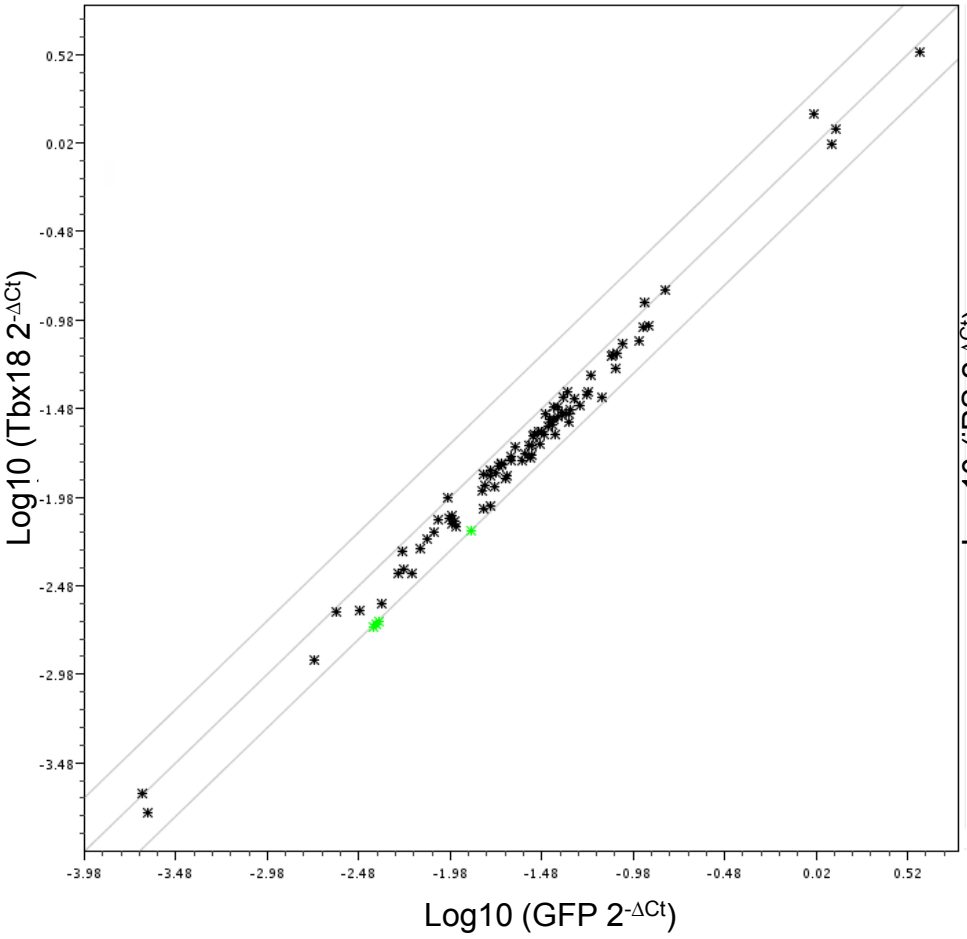


B iPS cells vs. parental Fibs

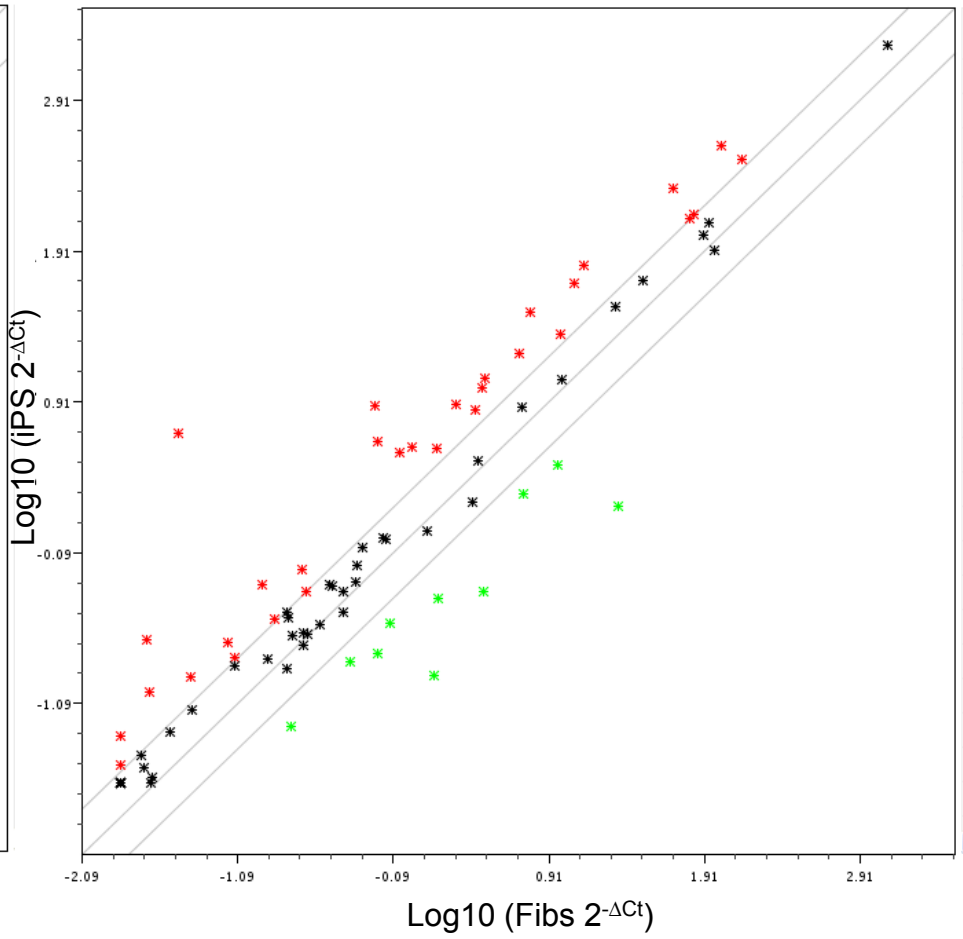

Supplementary Figure 10

Epigenetic Chromatin Remodeling Factors: RT-PCR array

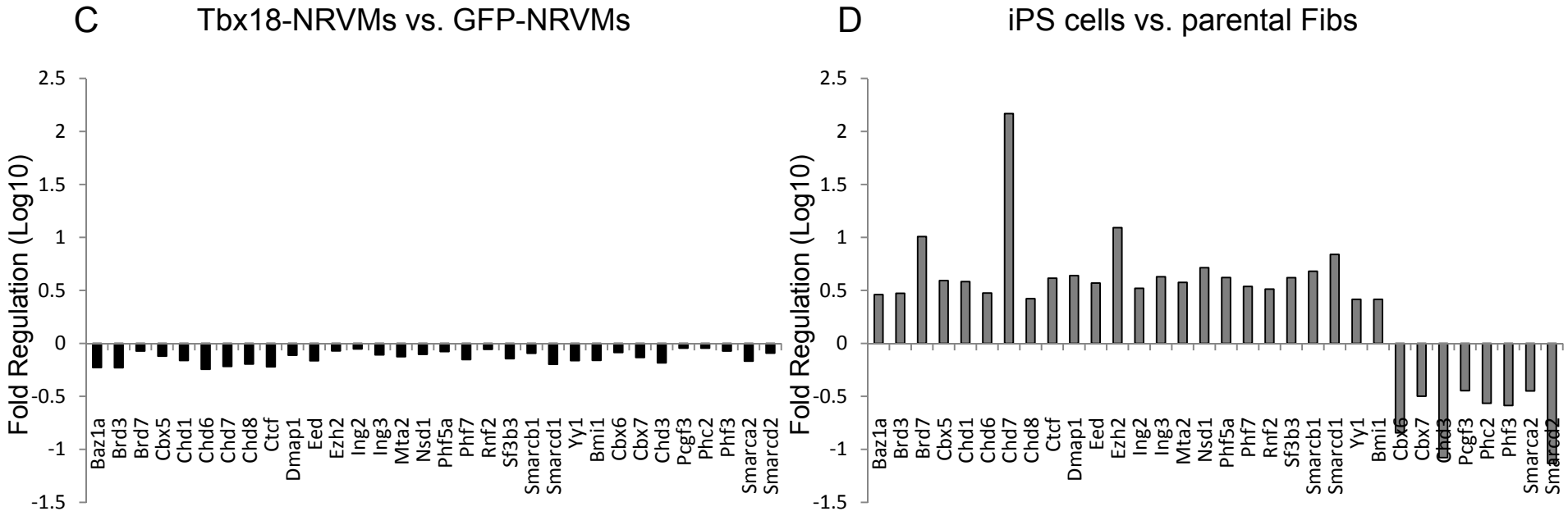

**Supplementary Figure 10.** Tbx18 does not cause a widespread modification of chromatin remodeling factors further supporting the data that it induces reprogramming of lineage-specific genes rather than non-specific dedifferentiation to fetal cardiomyocytes. **A**. Scatter plot depicts little changes to expression of the genes related chromatin remodeling in Tbx18-NRVMs compared to GFP-NRVMs. B. As a positive control, human induced pluripotent stem cells (iPSCs) were compared to the parental fibroblasts, demonstrating extensive up- or down-regulation of chromatin remodeling epigenetic markers in iPSCs. Fold-changes in specific genes are represented as bar graphs for Tbx18 (relative to GFP) and iPSCs (relative to parental fibroblasts) in C and D, respectively.

Supplementary Figure 11

Stem cell specific markers: RT-PCR array

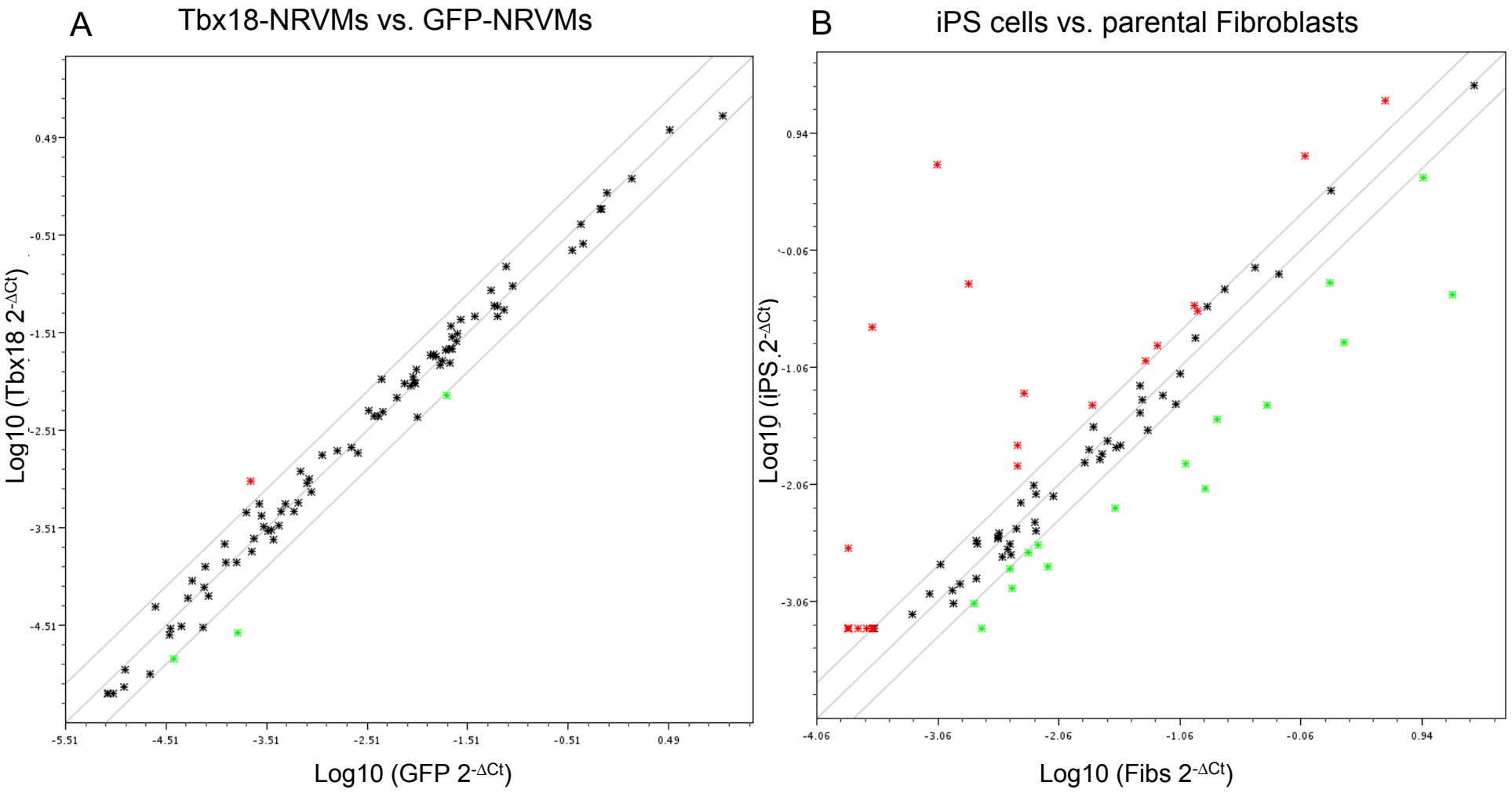

Supplementary Figure 11

Stem cell specific markers: RT-PCR array

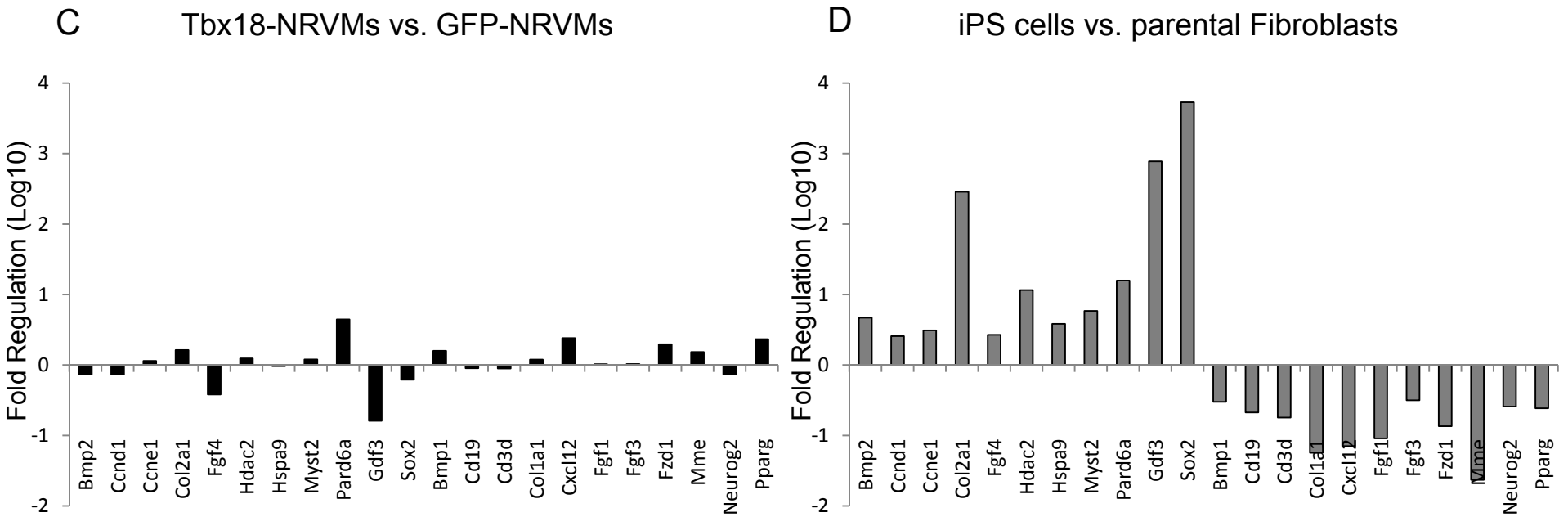

**Supplementary Figure 11**. RT-PCR array of 84 gene transcripts related to related to the identification, growth and differentiation of stem cells. **A**. Scatter plot depicts no discernible changes to transcript levels related to stemness in Tbx18-NRVMs compared to control. B. Human induced pluripotent stem cells (iPSCs) were compared to its parental fibroblasts, which demonstrate upregulation (red asterisks) of stemness and downregulation (green asterisks) of differentiation markers in iPSCs compared to the parental fibroblasts. Fold-changes in specific genes are represented as bar graphs for Tbx18 (relative to GFP) and iPSCs (relative to parental fibroblasts) in C and D, respectively.

# Supplementary Figure 12

A

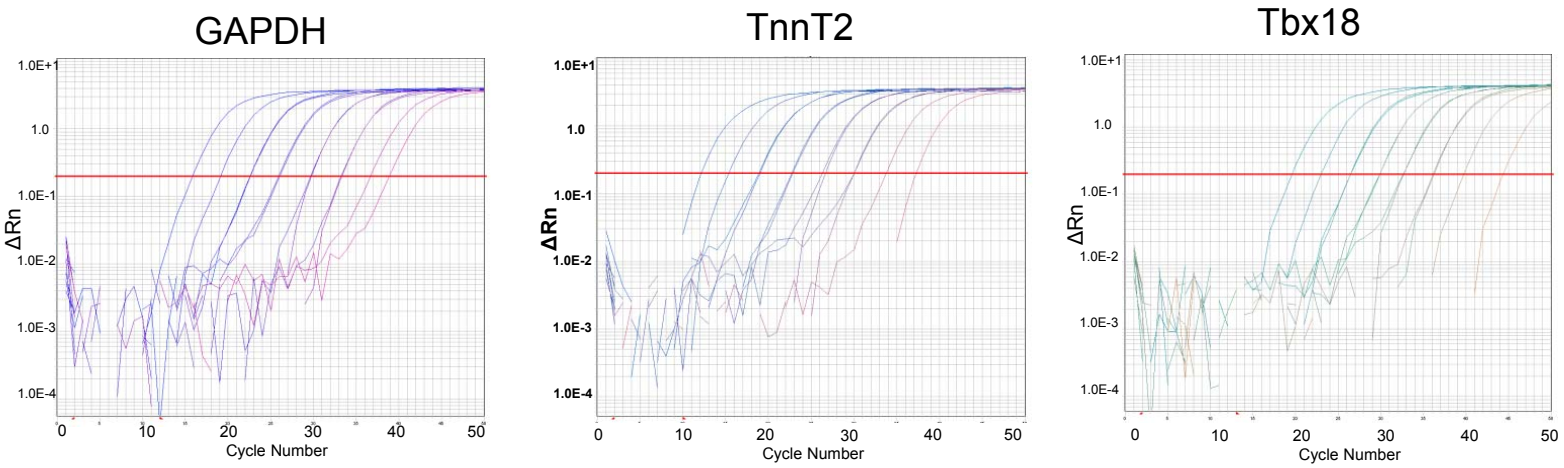


B

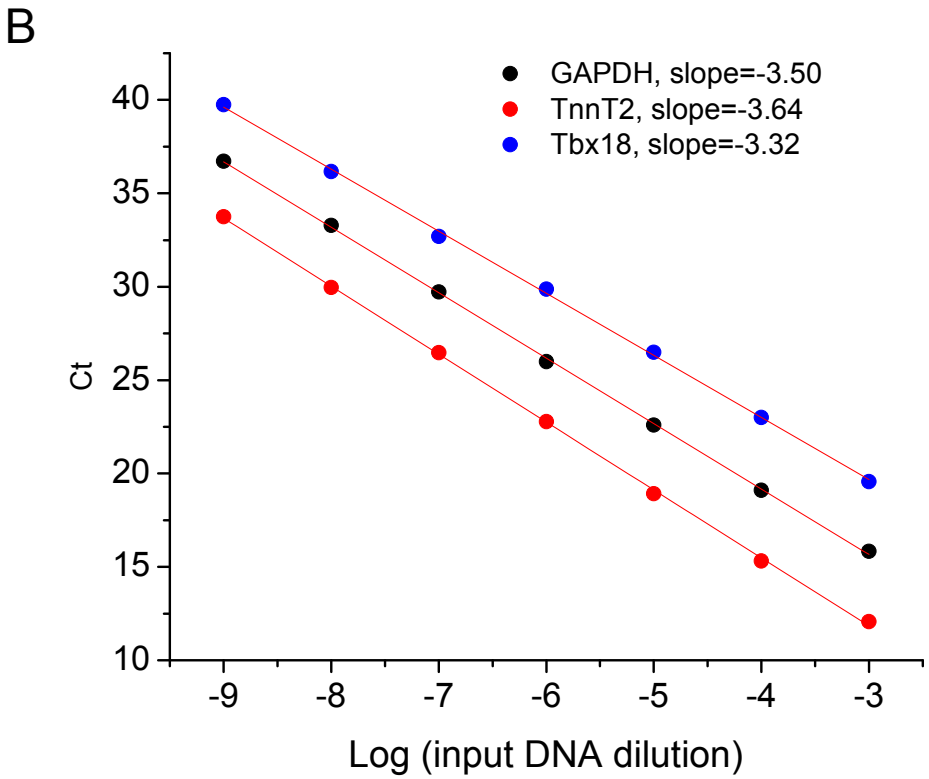

**Supplementary Figure 12**. **A**. Raw traces for constructing the standard curve of quantitative real-time PCR reactions with primer sets for GAPDH (left), TnnT2 (middle), and Tbx18 (right). Individuals traces in each panel were obtained with a serial dilution ($10^{-10}$ to $10^{-3}$) of input DNA templates. **B**. Plots of threshold cycle (Ct) vs. input DNA template dilution for GAPDH (black dots), TnnT2 (red dots), and Tbx18 (blue dots). Red lines indicate linear fittings (y=a+b*x), from which slope values were derived.